Hindawi
Oxidative Medicine and Cellular Longevity
Volume 2022, Article ID 2792348, 18 pages
https://doi.org/10.1155/2022/2792348

Research Article

Hydrogen Sulfide Attenuates the Cognitive Dysfunction in Parkinson's Disease Rats via Promoting Hippocampal Microglia M2 Polarization by Enhancement of Hippocampal Warburg Effect

Qing Tian,[1] **Hui-Ling Tang**,[1,2] **Yi-Yun Tang**,[1] **Ping Zhang**,[2] **Xuan Kang**,[1,3] **Wei Zou**,[2] **and Xiao-Qing Tang**[1,3]

[1]*Hengyang Key Laboratory of Neurodegeneration and Cognitive Impairment, Institute of Neuroscience, Hengyang Medical School, University of South China, Hengyang, 421001 Hunan, China*
[2]*The Affiliated Nanhua Hospital, Department of Neurology, Hengyang Medical School, University of South China, Hengyang, 421001 Hunan, China*
[3]*The First Affiliated Hospital, Institute of Neurology, Hengyang Medical School, University of South China, Hengyang, 421001 Hunan, China*

Correspondence should be addressed to Ping Zhang; zhangp-usc@foxmail.com and Xiao-Qing Tang; tangxq-usc@qq.com

Qing Tian, Hui-Ling Tang, and Yi-Yun Tang contributed equally to this work.

Received 12 August 2021; Revised 6 November 2021; Accepted 15 November 2021; Published 4 January 2022

Academic Editor: Fushun Wang

Identification of innovative therapeutic targets for the treatment of cognitive impairment in Parkinson's disease (PD) is urgently needed. Hydrogen sulfide (H_2S) plays an important role in cognitive function. Therefore, this work is aimed at investigating whether H_2S attenuates the cognitive impairment in PD and the underlying mechanisms. In the rotenone- (ROT-) established PD rat model, NaHS (a donor of H_2S) attenuated the cognitive impairment and promoted microglia polarization from M1 towards M2 in the hippocampus of PD rats. NaHS also dramatically upregulated the Warburg effect in the hippocampus of PD rats. 2-Deoxyglucose (2-DG, an inhibitor of the Warburg effect) abolished NaHS-upregulated Warburg effect in the hippocampus of PD rats. Moreover, the inhibited hippocampal Warburg effect by 2-DG abrogated H_2S-excited the enhancement of hippocampal microglia M2 polarization and the improvement of cognitive function in ROT-exposed rats. Our data demonstrated that H_2S inhibits the cognitive dysfunction in PD via promoting microglia M2 polarization by enhancement of hippocampal Warburg effect.

1. Introduction

Parkinson's disease (PD), characterized by the loss of dopaminergic neurons, is a common neurodegenerative disease [1, 2]. PD is defined primarily as a movement disorder, with the typical dopamine-related motor symptoms being resting tremor, rigidity, bradykinesia, and postural instability. However, a wide variety of nonmotor symptoms are commonly observed in patients with PD [3]. The cognitive dysfunction is a frequent important nonmotor symptom encountered in PD patients [3]. It has been reported that the lesioned hippocampus, a temporal lobe structure, leads to memory dysfunction [4, 5]. Furthermore, aerobic exercise training is effective at reversing hippocampal volume loss, which is accompanied by improved memory function [6]. As reported that verbal memory deficient in recall and recognition is associated with atrophy of the hippocampus in newly diagnosed PD patients [7], recent advancement also observed hippocampal subfield atrophy of CA1 in participants who progressed to PD dementia [8]. All of these reflect an intimate relationship between hippocampal dysfunction and cognitive impairment in PD. However, there is no

effective strategy to prevent the cognitive impairment in PD. Hydrogen sulfide (H_2S), well known as a neuromodulator [9], alleviates cognitive deficits caused by multiple risk factors [10–12]. Our previous work demonstrated that the cognitive impairment in formaldehyde- or homocysteine-exposed rats is related to the disturbance of endogenous H_2S [13, 14] and that supplementation of exogenous H_2S prevents the cognitive impairment in homocysteine- [15, 16], chronic restrain stress- [17], and streptozotocin- [18] exposed rats. Collectively, the antagonistic action of H_2S on cognitive dysfunction is widely recognized. Thus, it seems reasonable to speculate the therapeutic potential of H_2S for the cognitive deficit in PD.

Microglia is the primary immune cells in the brain, acting as immune surveillance and host defense. Accumulating evidence has reported that microglia regulate neurodevelopment and synaptic plasticity [19, 20]. Like macrophages, microglia are designated classically activated (M1) and alternatively activated (M2) phenotypes [21]. M1 microglia release proinflammatory cytokines to destroy neurons, and contrarily, M2 microglia secrete neuroprotective mediators and trophic factors. It has been confirmed that promoting microglia M2 polarization enhances α-synuclein clearance in PD [22]. Furthermore, maintaining the balance of M1 and M2 is crucial to alleviate cognitive disorder in schizophrenia [23] and enhancing M2 polarization mitigates Aβ-caused cognitive dysfunction [24]. Additionally, H_2S exerts a regulatory role in microglia polarization [25, 26]. Thus, to understand the mechanism underlying H_2S-promoted cognitive function in PD, we investigated whether H_2S skews M1 microglia polarization toward M2 activation.

The Warburg effect, also known as aerobic glycolysis, involves the metabolism of glucose to supply ATP and secrete lactate via glycolysis under aerobic conditions. Otto Warburg's work first reported that cancer cells have a propensity to metabolize glucose via glycolysis despite oxygen availability [27]. Interestingly, the Warburg effect also plays vital regulatory roles in the function of the brain, supporting the molecular demands of neuronal proliferation in embryonic development, promoting the maturational changes of neurons in postnatal development, and is responsible for changes at the synapse in adulthood [28, 29]. Moreover, lactate, a metabolite of the Warburg effect, exerts a regulatory role in synaptic plasticity by enhancing the expressions of Egr-1 and c-Fos. A recent study reported that lactate is required for long-term potentiation (LTP) formation [30], providing a new insight into the mechanism of cognition [31, 32]. These observations prompted us to raise the question of whether the Warburg effect mediates the antagonistic role of H_2S in the cognitive deficit in PD.

In this study, we found that H_2S alleviated the cognitive impairment, promoted hippocampal microglia M2 polarization, and enhanced hippocampal Warburg effect in the rotenone-induced PD rats. Furthermore, inhibition of the hippocampal Warburg effect abrogated H_2S-exerted protection against the cognitive disorder and promotion of hippocampal microglia M2 polarization in PD rats. Our findings demonstrated that H_2S enhances hippocampal Warburg effect, leading to promote microglia M2 polarization, which in turn prevents the cognitive disorder in PD.

2. Materials and Methods

2.1. Reagents. NaHS, rotenone (ROT), 2-deoxyglucose (2-DG), sunflower seed oil, and a lactate assay kit were purchased from Sigma (MO, USA). The primary antibodies against hexokinase II (HKII), pyruvate kinase M2 (PKM2), pyruvate dehydrogenase kinase 1 (PDK-1), pyruvate dehydrogenase (PDH), lactate dehydrogenase kinase A (LDHA), and arginase-1 (Arg-1) were obtained from Cell Signaling Technology (MA, USA). The primary antibodies against chitinase 3-like 3 (Ym-1) and inducible nitric oxide synthase (iNOS) and the Griess assay kit were obtained from Abcam (CA, USA). The Rat TGF-β1 ELISA kit was purchased from BioVision (CA, USA), and the Rat IL-4 ELISA Kit and Rat IL-1β ELISA Kit were purchased from ABclonal (Wuhan, China).

2.2. PD Animal Model and Animal Dosing. The adult male Sprague-Dawley (SD) rats weighing 260–280 g were obtained from SJA Lab. Each group contained 15 rats and each rat was housed individually with free access to food and water. The room humidity was controlled at 40%–46%, and the temperature was controlled within 22–26 ˚C. SD rats were exposed to ROT (2 mg/kg, s.c.) for 5 w to mimic the PD model [33]. After habituating to this new housing environment for 1 w, rats were administered NaHS (30 and 100 μmol/kg, i.p.) for 1 w. Subsequently, rats were exposed to ROT via subcutaneous injection for 5 w and NaHS for 3 w simultaneously. In the 3rd week of injecting ROT, rats were cotreated with 2-DG (3 μg/w, i.c.v.) for 3 w. After performing behavioral tests, the brains of rats were collected under euthanasia (Figure 1). All experiments strictly complied with the *Guide for the Care and Use of Laboratory Animals* of the National Institutes of Health and were approved by the Animal Use and Protection Committee of the University of South China.

2.3. Intracerebroventricular Injection. Under deep anesthesia using pentobarbital sodium (45 mg/kg), animals were fixed on the stereotaxic apparatus for the following operation. The hair from the top of the skull was removed, fully exposing the bregma. The position of the right lateral ventricle was determined according to the following coordinates: AP, −1.0 mm; ML, −2.0 mm; DV, −4.0 mm. Then, the aseptic cannula was implanted into this location for drug administration. After surgery, penicillin was administered for 3 consecutive days to prevent infection. Rats were recovered for 1 w. 2-DG was administered into the lateral ventricle along the cannula using a microsyringe. The needle was removed slowly and kept halfway in for an extra 2 min to ensure complete delivery of the drug.

2.4. Y-Maze Test. The Y-maze test was used to evaluate the learning and memory of rats. The experimental apparatus consisted of three identical labeled arms (A, B, and C) at equal angles. At the beginning of the test, the rat was placed in the intersection of the three arms to explore freely for 5 min. The sequence and number of the rat entries into each arm were recorded. The rat entering different arms in turn during three consecutive chances was marked as a correct sequence (for example, ABC, BAC, or ACB, but not ABA

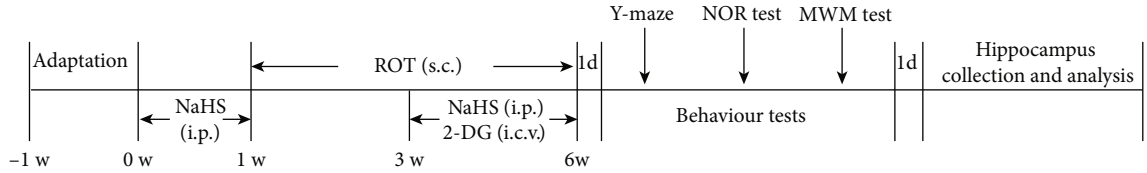

Figure 1: Schematic of experimental design. i.p.: intraperitoneal; s.c.: subcutaneous; i.c.v.: intracerebroventricular.

and etc.). Once the rat completed the test, the three arms and the bottom of the apparatus were swept and wiped using 70% alcohol to eliminate the potential influence of odors and residues on experimental data. The alternation performance was calculated to evaluate the spatial differentiation memory of rats.

2.5. Novel Object Recognition (NOR) Test. The open-field box that was used in this experiment was 50 cm × 40 cm × 30 cm. To avoid being pushed or bitten by rats, the recognized objects were cylinders and tubes with a certain weight as well as hardness. The whole experiment was divided into three periods: the adaptation period, training period, and testing period. The adaptation period lasted for 2 d. All rats were introduced to the test box from the fixed position and were adapted to this new environment for 5 min without objects. During the training period, the rat entered the box with two identical objects from a fixed position, and the time that the rat spent exploring each of the two objects was recorded. After an hour-long retention interval, the rat was reintroduced to the test box, with one familiar object replaced by one novel object, and the time that the rat spent exploring each of the two objects over the course of 5 min was recorded. Touching, sniffing, and direct attention to an object rather than climbing or chewing objects were defined as exploratory behaviors. A distance between the nose and object within 2 cm was also regarded as exploratory behavior. The discrimination index was calculated to reflect the cognitive function of the rat, which was defined by the following equation: discrimination index = [(time spent on familiar object − time spent on novel object)/(time spent on familiar object + time spent on novel object)] × 100.

2.6. Morris Water Maze (MWM) Test. The MWM system mainly includes a circular pool with water and a hidden platform. The pool was divided into four quadrants, and the target quadrant was defined as the platform positioned in the center of this area. In the acquisition phase (days 1–5), rats were randomly introduced into the pool from different quadrants to search for the hidden platform in four trials per day with a 20-minute interval. The maximum swimming time for each rat was 120 s in each trial; otherwise, rats were guided to the hidden platform and allowed to stay there for 20 s. The swimming route and latency to the platform were tracked by the MT-200 Morris Image Motion System. In the probe phase (day 7), rats were reintroduced to the pool without a platform from the opposite position to the target quadrant. The time spent swimming in the target quadrant and the number of crossing the target platform of rats were recorded over the course of 120 s. Following the probe test, rats were subjected to the visible platform test to rule out possible deficits in vision and motor function, which may impact experimental data. The platform was replaced opposite to the target quadrant and was 2 cm higher above the water. Rats were reintroduced to the pool from the side opposite to the platform, and the escape latency and average speed were recorded.

2.7. Western Blot Analysis. After all behavioral tests were completed, rats were sacrificed, and hippocampal tissues of the brain were dissected. Then, hippocampal tissues were homogenized using lysis buffer, and supernatant was collected after centrifugation. The protein content was measured by a BCA protein assay kit. The prepared samples were added into sodium dodecyl sulfate-polyamide gel for electrophoresis and subsequently transferred to the polyvinylidene fluoride membrane. The membranes were blocked using 5% skim milk in Tris-buffered saline containing 0.1% Tween-20 (TBST). Two hours later, these were incubated with primary antibodies overnight at 4°C and subsequently washed 10 min in TBST followed by incubation with corresponding secondary antibodies for 2 h. Finally, membranes were visualized by an enhanced chemiluminescence system (BeyoECL Plus kit, Beyotime). AlphaImager 2200 software was used to calculate the signal of immunoblot.

2.8. Determination of Lactate Level in the Hippocampus. The level of lactate was analyzed by a lactate assay kit. In this assay, the lactate content was determined by a colorimetric product in an enzymatic assay. Briefly, hippocampal tissues were homogenized in 4 volumes of the Lactate Assay Buffer and centrifuged at 13,000 × g for 10 min. Supernatants were collected and deproteinized to remove lactate dehydrogenase. Subsequently, 3 μl of each sample was added into a 96-well plate, and Lactate Assay Buffer was supplemented to a final volume of 50 μl per well. After that, 50 μl of Master Reaction Mix (46 μl Lactate Assay Buffer, 2 μl Lactate Enzyme Mix, and 2 μl Lactate Probe) was added to each well and incubated at room temperature without light. Thirty minutes later, the absorbance at 450 nm was measured under a microplate reader. The content of lactate in samples was determined by a formula and a standard curve referencing the manufacturer's instructions.

2.9. Immunofluorescence Staining. After fixing in 4% paraformaldehyde, brain samples were dehydrated and subsequently embedded into paraffin. The paraffin-embedded sections were treated with citric acid-containing buffer and coated in 3% H_2O_2 for 10 min at 37°C. Following blockages to eliminate nonspecific staining, sections were incubated

with the primary antibodies at 4°C overnight. After washing in PBS three times for 5 min, sections were incubated with corresponding secondary antibodies in the dark at 37°C to visualize the fluorescent signal. The nuclei were visualized using DAPI staining solution for 1 h without light. While coverslips were mounted, stained sections were visualized and photographed under a microscope.

2.10. Enzyme-Linked Immunosorbent Assay (ELISA). The contents of TGF-β1, IL-1β, and IL-4 were detected by the corresponding ELISA kits. According to the manufacturer's instructions, supernatants of tissues were collected via lysis and centrifugation. Samples were added into the microplate stripe wells and then mixed with HRP-labeled antibody. Microplate was coated with microplate sealers and incubated at 37°C. After washing, substrate A and substrate B were added separately to each well to incubate in the dark and then supplemented with stop solution. The optical density at 450 nm was measured within 15 min using a microplate reader.

2.11. Griess Assay. The level of NO was detected using a Griess assay kit. Supernatant was collected and added into a 96-well plate. Solution I and solution II were added, mixed, and then incubated for 20 min without light. The optical density at 540 nm was measured using a microplate reader.

2.12. Statistical Analysis. All data in this paper were obtained using SPSS 20 software and described as the mean ± S.E.M. The significance of intergroup differences was determined by one-way ANOVA. The variance and multiple comparisons were evaluated by LSD-t. $P < 0.05$ was set as the standard for a significant difference.

3. Results

3.1. H_2S Attenuates the Cognitive Impairment in ROT-Induced PD Rats. We explored the effect of H_2S on the cognitive disorder in ROT-induced PD rats using the Y-maze, NOR, and MWM tests.

In the Y-maze test, NaHS (a donor of H_2S) markedly increased the alternation performance in the ROT-exposed rats (Figure 2(a)). In addition, there was no significant difference in the number of total entries among experimental groups (Figure 2(b)).

In the NOR test, there was no significant difference in the total time spent exploring the two objects among the five groups during the training phase (Figure 3(a)) as well as testing phase (Figure 3(c)). However, the discrimination index in the testing phase was decreased in the ROT-exposed rats and dramatically elevated by treatment with NaHS (Figure 3(b)).

The MWM test was also used to explore the effect of H_2S on the declined learning and memory in the ROT-induced PD rats. In the acquisition phase of the MWM test, the swimming routes for searching for the platform were tortuous and complicated for all groups on the first training day, while NaHS significantly simplified the search routes of ROT-exposed rats on the fifth day (Figure 4(a)). Furthermore, ROT treatment lengthened the latency to find the platform compared to the control group (Figure 4(b)), which was significantly reduced by NaHS supplementation (Figure 4(c)). NaHS treatment alone showed no impact on the normal rats to find the platform (Figure 4(d)). In the probe trial phase of the MWM test, NaHS significantly increased the number across the target platform (Figure 4(e)) and the time spent in the target quadrant (Figure 4(f)) among the ROT-exposed rats. In the visible platform phase of the MWM test, no significant differences in the escape latency (Figure 4(g)) and the average speed (Figure 4(h)) were observed among groups.

Together, these findings indicated that H_2S attenuates the cognitive impairment in the ROT-induced PD rats.

3.2. H_2S Promotes Microglia Polarization from M1 to M2 in the Hippocampus of ROT-Exposed Rats. Next, we assessed the effect of H_2S on microglia polarization in the hippocampus of ROT-exposed rats. The bright fluorescence of Iba1 in ROT-exposed rats exhibited a reduced state after NaHS treatment (Figures 5(a) and 5(b)), indicating the inhibitory role of H_2S in microglia activation. The most important characteristic of microglia polarization is the phenotype alteration. We found that H_2S inhibited M1 polarization of microglia, which was characterized by the decreased expression of iNOS (Figure 5(c)) and the secretions of NO (Figure 5(d)) and IL-1β (Figure 5(e)) in the hippocampus of rats cotreatment with ROT and NaHS. More strikingly, H_2S accelerated microglia polarization to M2 phenotype, featured with the upregulated protein expressions of Arg-1 (Figure 5(f)) as well as Ym-1 (Figure 5(g)) and the increased secretions of TGF-β1 (Figure 5(h)) as well as IL-4 (Figure 5(i)) in the hippocampus of rats cotreatment with ROT and NaHS. These data indicated that H_2S promotes microglia M2 polarization in the hippocampus of ROT-induced PD rats.

3.3. H_2S Upregulates the Hippocampal Warburg Effect in the ROT-Exposed Rats. To investigate the role of H_2S in the hippocampal Warburg effect of rats, we measured the hallmarks related to the Warburg effect in the hippocampus. NaHS markedly upregulated the expressions of HKII (Figure 6(a)), PKM2 (Figure 6(b)), PDK-1 (Figure 6(c)), and LDHA (Figure 6(d)), as well as downregulated the expression of PDH (Figure 6(e)) in the hippocampus of ROT-exposed rats. Moreover, the content of lactate decreased in the hippocampus of ROT-treated rats, which was increased by treatment with NaHS (Figure 6(f)). Taken together, these findings indicated that H_2S enhances the Warburg effect in the hippocampus of ROT-treated rats.

3.4. 2-DG Prevents the Upregulatory Role of H_2S in the Hippocampal Warburg Effect of ROT-Exposed Rats. To investigate whether inhibited the hippocampal Warburg effect reverses the protection of H_2S against ROT-induced decline in cognitive function, we first investigated whether 2-DG (an inhibitor of the Warburg effect) [34, 35] abolished H_2S-enhanced Warburg effect in the hippocampus of ROT-exposed rats. 2-DG dramatically ameliorated NaHS-elicited upregulation in the expressions of HKII (Figure 7(a)), PKM2 (Figure 7(b)), PDK-1 (Figure 7(c)), and LDHA (Figure 7(d)) as well as downregulation in the expression of PDH (Figure 7(e)) in the hippocampus of ROT-exposed rats. Furthermore, 2-DG significantly reversed the role of

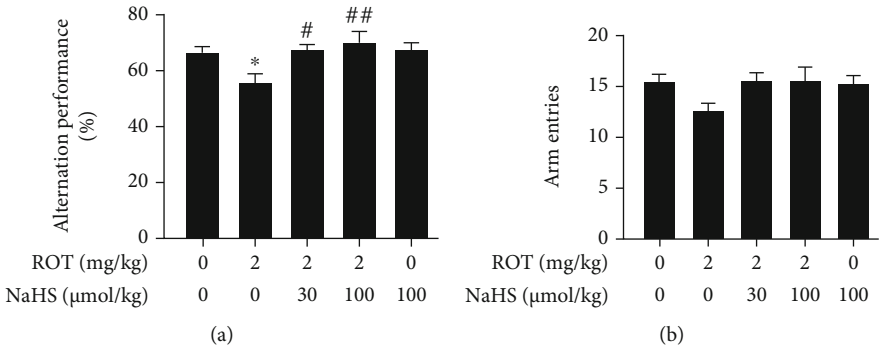

Figure 2: Effect of H_2S on the cognitive impairment of ROT-induced PD rats in the Y-maze test. After pretreatment with NaHS (30 and 100 μmol/kg, i.p.) for 1 w, SD rats were injected with ROT (2 mg/kg, s.c.) for 5 w and NaHS for 3 w simultaneously. All rats were subjected to the Y-maze test. The alternation performance (a) and the arm entries (b) over the course of 5 min were analyzed. Values are presented as the mean ± S.E.M. ($n = 9 – 15$). $^{*}P < 0.05$ vs. control group; $^{\#}P < 0.05$ and $^{\#\#}P < 0.01$ vs. ROT treatment alone group.

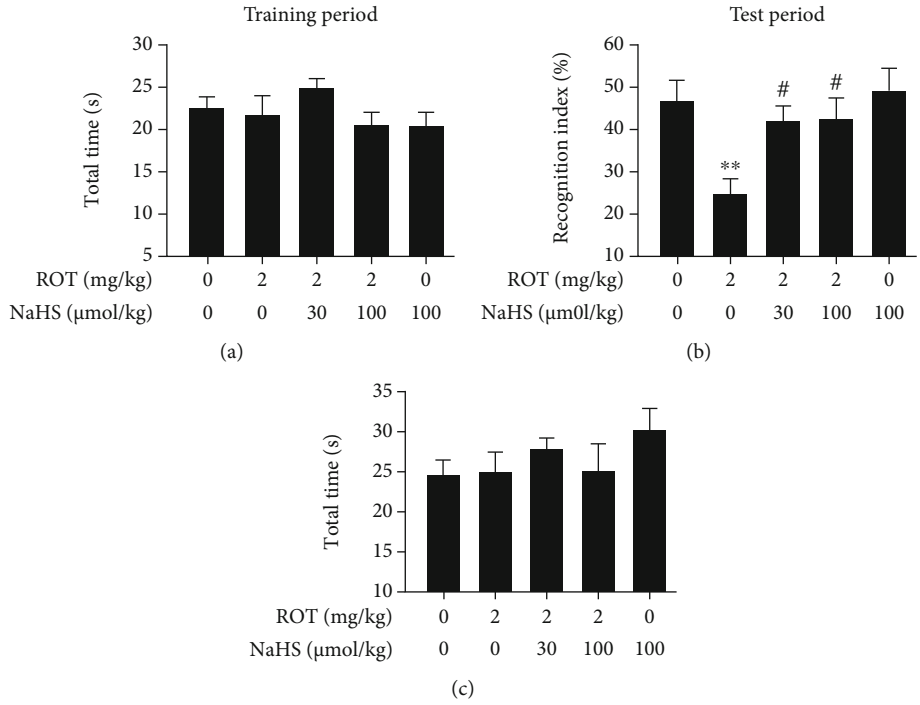

Figure 3: Effect of H_2S on the cognitive impairment of ROT-induced PD rats in the NOR test. After pretreatment with NaHS (30 and 100 μmol/kg, i.p.) for 1 w, SD rats were injected with ROT (2 mg/kg, s.c.) for 5 w and NaHS for 3 w simultaneously. Rats were subjected to the NOR test. The total time in the training period (a) and the recognition index (b) as well as total time (c) in the test period over the course of 5 min were assessed. Values are presented as the mean ± S.E.M. ($n = 9 – 15$). $^{**}P < 0.01$ vs. control group; $^{\#}P < 0.05$ vs. ROT exposure alone group.

NaHS in enhancing the hippocampal lactate level of ROT-exposed rats (Figure 7(f)). These data indicated that 2-DG prevents H_2S-enhanced Warburg effect in the hippocampus of ROT-induced PD rats.

3.5. Inhibited Hippocampal Warburg Effect Reverses H_2S-Attenuated Cognitive Dysfunction of PD Rats. To confirm the mediatory role of hippocampal Warburg effect in H_2S-promoted cognitive function of PD rats, we further explored whether inhibited hippocampal Warburg effect by 2-DG abolishes H_2S-promoted cognitive function in the ROT-treated rats.

In the Y-maze test, 2-DG dramatically reversed the upregulatory effect of NaHS on the alternative performance of ROT-treated rats (Figure 8(a)). The total entries showed no significant difference among the groups (Figure 8(b)).

In the NOR test, 2-DG greatly decreased the recognition index of rats cotreated with ROT and NaHS (Figure 9(b)). There was no significant difference in the total time spent in exploring objects (Figures 9(a) and 9(c)).

In the acquisition phase of the MWM test, 2-DG significantly complicated the swimming routes (Figure 10(a)) and extended the latency to find the platform in the rats cotreated

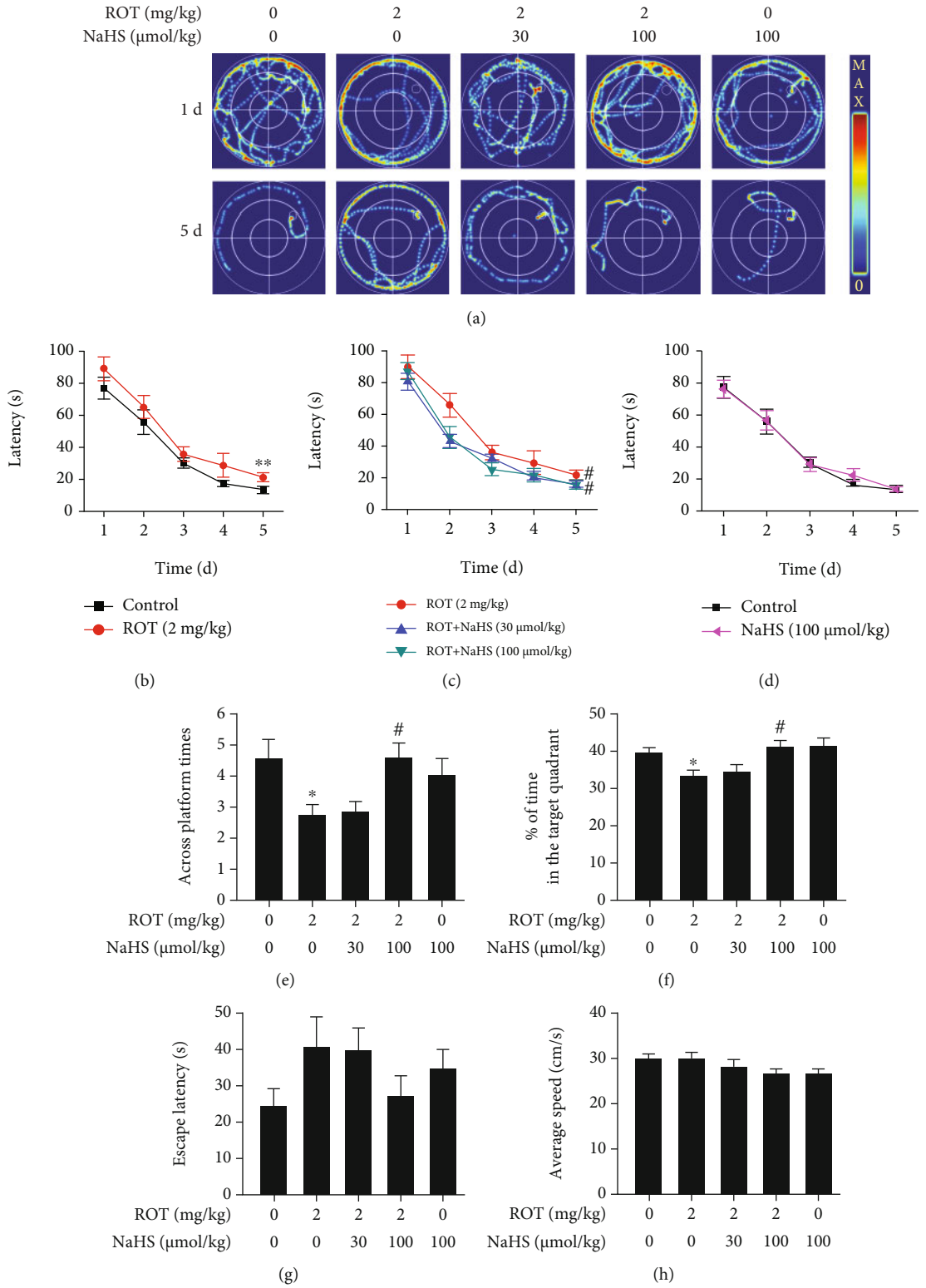

FIGURE 4: Effect of H_2S on the cognitive impairment of ROT-induced PD rats in the MWM test. After pretreated with NaHS (30 and 100 μmol/kg, i.p.) for 1 w, SD rats were injected with ROT (2 mg/kg, s.c.) for 5 w and NaHS for 3 w simultaneously. Rats were then subjected to the MWM test. The representative swimming routes of one rat for each group in searching for the platform were recorded on the 1st and 5th training days (a). The latency to find the platform in the acquisition phase was recorded (b–d). The number of crossing the platform (e) and the percentage of time spent in the target quadrant (f) in the probe trial phase were assessed. The escape latency (g) and average speed (h) of rats in the visible platform phase were recorded. Values are presented as the mean ± S.E.M. ($n = 9 - 15$). $^{*}P < 0.05$ and $^{**}P < 0.01$ vs. control group; $^{\#}P < 0.05$ vs. ROT exposure alone group.

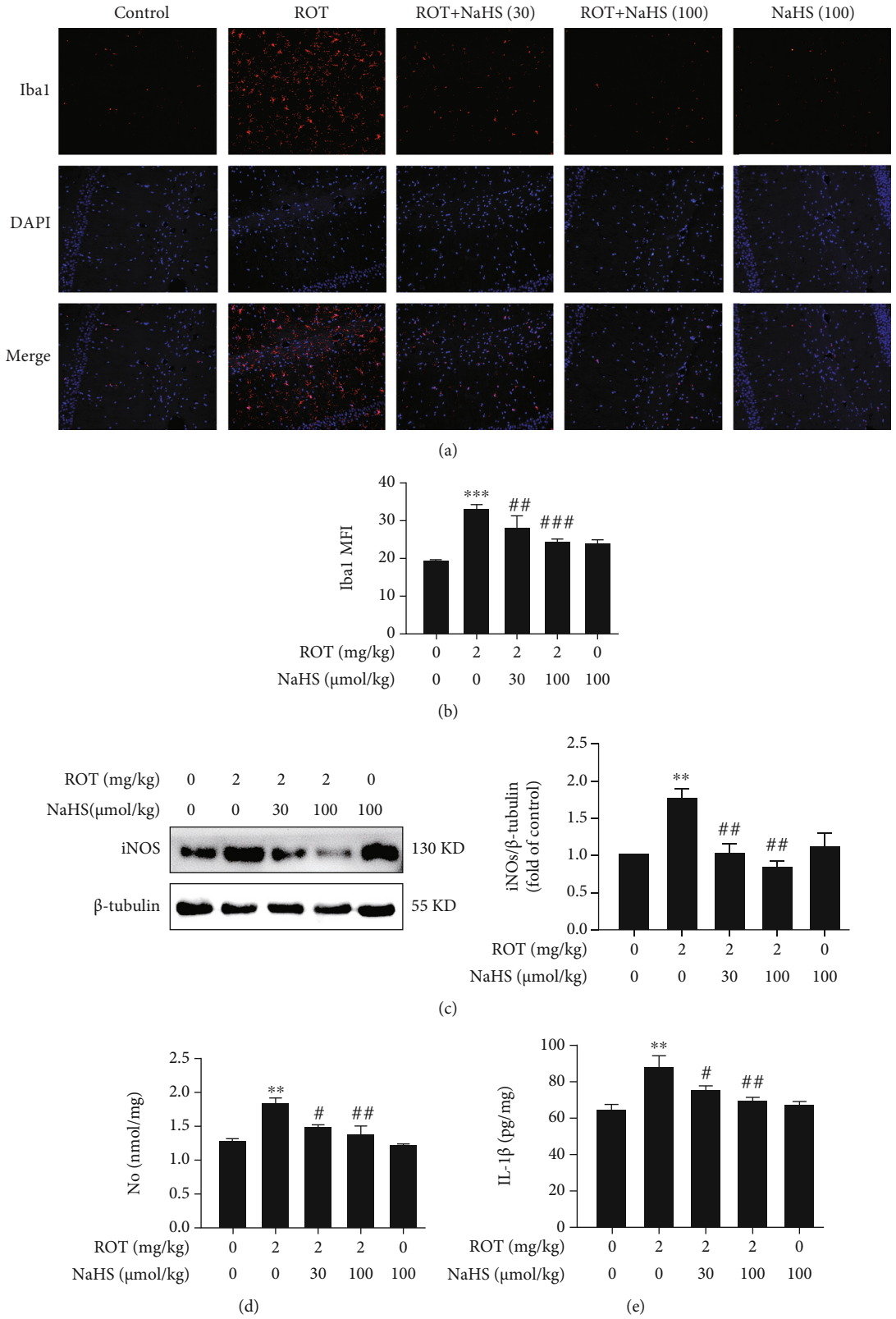

Figure 5: Continued.

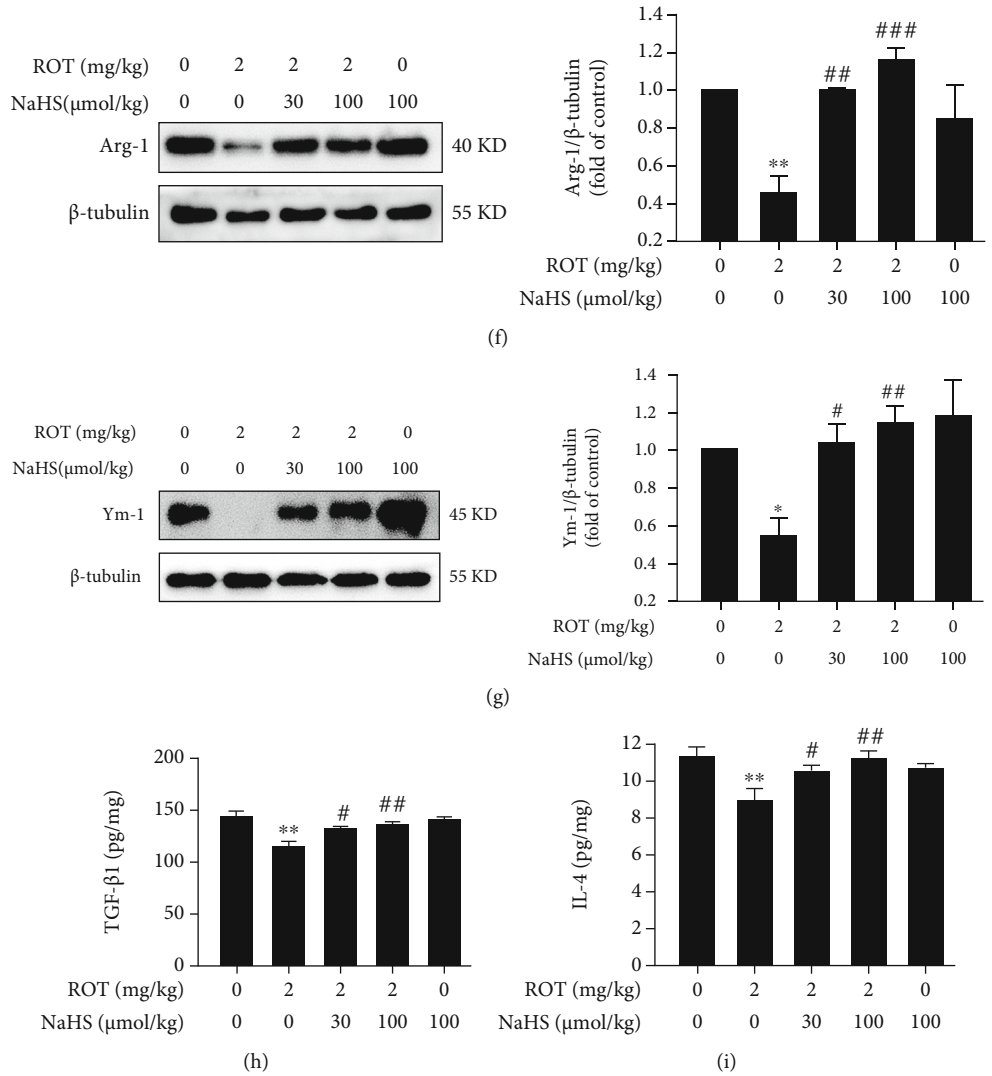

Figure 5: Effect of H_2S on microglia polarization in the hippocampus of ROT-induced PD rats. After pretreatment with NaHS (30 and 100 μmol/kg, i.p.) for 1 w, SD rats were injected with ROT (2 mg/kg, s.c.) for 5 w and NaHS for 3 w simultaneously. Representative images of activated microglia (a). Quantification of mean fluorescence intensity (MFI) of Iba1 (b). The nuclei were stained by DAPI (blue), and the activated microglia was stained by Iba1 (red). Magnification, 20x. The expressions of iNOS (c), Arg-1 (f), and Ym-1 (g) were measured by western blot. The level of NO (d) was measured by the Griess assay kit. The contents of IL-1β (e), TGF-β1 (h), and IL-4 (i) were detected by ELISA. Values are presented as the mean ± S.E.M. ($n = 3$). $^{*}P < 0.05$, $^{**}P < 0.01$, and $^{***}P < 0.001$ vs. control group; $^{\#}P < 0.05$, $^{\#\#}P < 0.01$, and $^{\#\#\#}P < 0.001$ vs. ROT treatment alone group.

with ROT and NaHS (Figures 10(b)–10(e)). In the probe trial of the MWM test, 2-DG decreased the number across the target platform (Figure 10(f)) and the percentage of time spent in the target quadrant (Figure 10(g)) of the rats cotreated with ROT and NaHS. The visible platform phase in the MWM test showed no significance in the escape latency (Figure 10(h)) or the average speed (Figure 10(i)) among all groups.

Taken together, suppression in the hippocampal Warburg effect abrogated the protection of H_2S against the cognitive impairment in ROT-exerted PD rats.

3.6. Inhibited Hippocampal Warburg Effect Reverses H_2S-Promoted Microglia M2 Polarization in the Hippocampus of ROT-Induced PD Rats. Next, we explored whether inhibited hippocampal Warburg effect by 2-DG reverses H_2S-promoted microglia M2 polarization in the hippocampus of ROT-induced PD rats. Our data showed that 2-DG increased the fluorescence intensity of Iba-1 (Figures 11(a) and 11(b)) in the rats cotreated with ROT and NaHS, indicating that inhibited hippocampal Warburg effect by 2-DG restored the microglia activation. Additionally, 2-DG supplementation led to increases in the expression of iNOS (Figure 11(c)) as well as the contents of NO (Figure 11(d)) and IL-1β (Figure 11(e)) in the rats cotreated with ROT and NaHS, indicating that inhibited hippocampal Warburg effect by 2-DG enhanced M1 polarization. Conversely, 2-DG reduced the expressions of Arg-1(Figure 11(f)) and Ym-1 (Figure 11(g)) as well as the contents of TGF-β1 (Figure 11(h)) and IL-4 (Figure 11(i)) in the rats

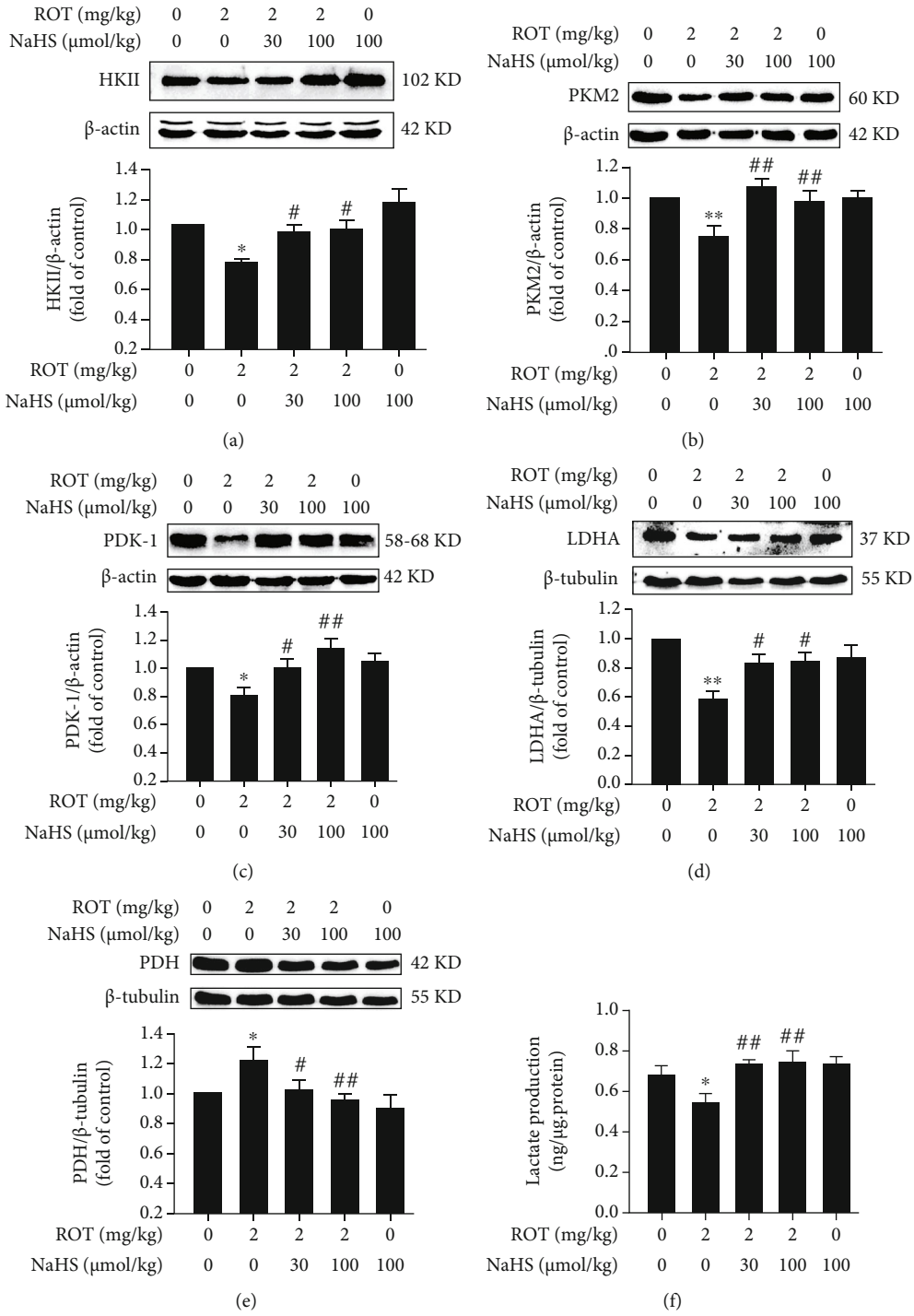

Figure 6: Effect of H_2S on the Warburg effect in the hippocampus of ROT-induced PD rats. After pretreatment with NaHS (30 and 100 μmol/kg, i.p.) for 1 w, SD rats were injected with ROT (2 mg/kg, s.c.) for 5 w and NaHS for 3 w simultaneously. The expressions of HKII (a), PKM2 (b), PDK-1 (c), LDHA (d), and PDH (e) in the hippocampus were detected by western blot. The content of lactate (f) in the hippocampus was tested by a lactate assay kit. Values are presented as the mean ± S.E.M. ($n = 3$). $^{*}P < 0.05$ and $^{**}P < 0.01$ vs. control group; $^{\#}P < 0.05$ and $^{\#\#}P < 0.01$ vs. ROT treatment alone group.

cotreated with ROT and NaHS, indicating inhibited hippocampal Warburg effect by 2-DG reduced M2 polarization. These results demonstrated that inhibited hippocampal Warburg effect abolishes H_2S-accelerated microglia M2 polarization in the hippocampus of ROT-induced PD rats.

4. Discussion

How to effectively ameliorate cognitive impairment is a huge problem that needs to be solved to improve the life quality of PD patients. In this study, we demonstrated that H_2S

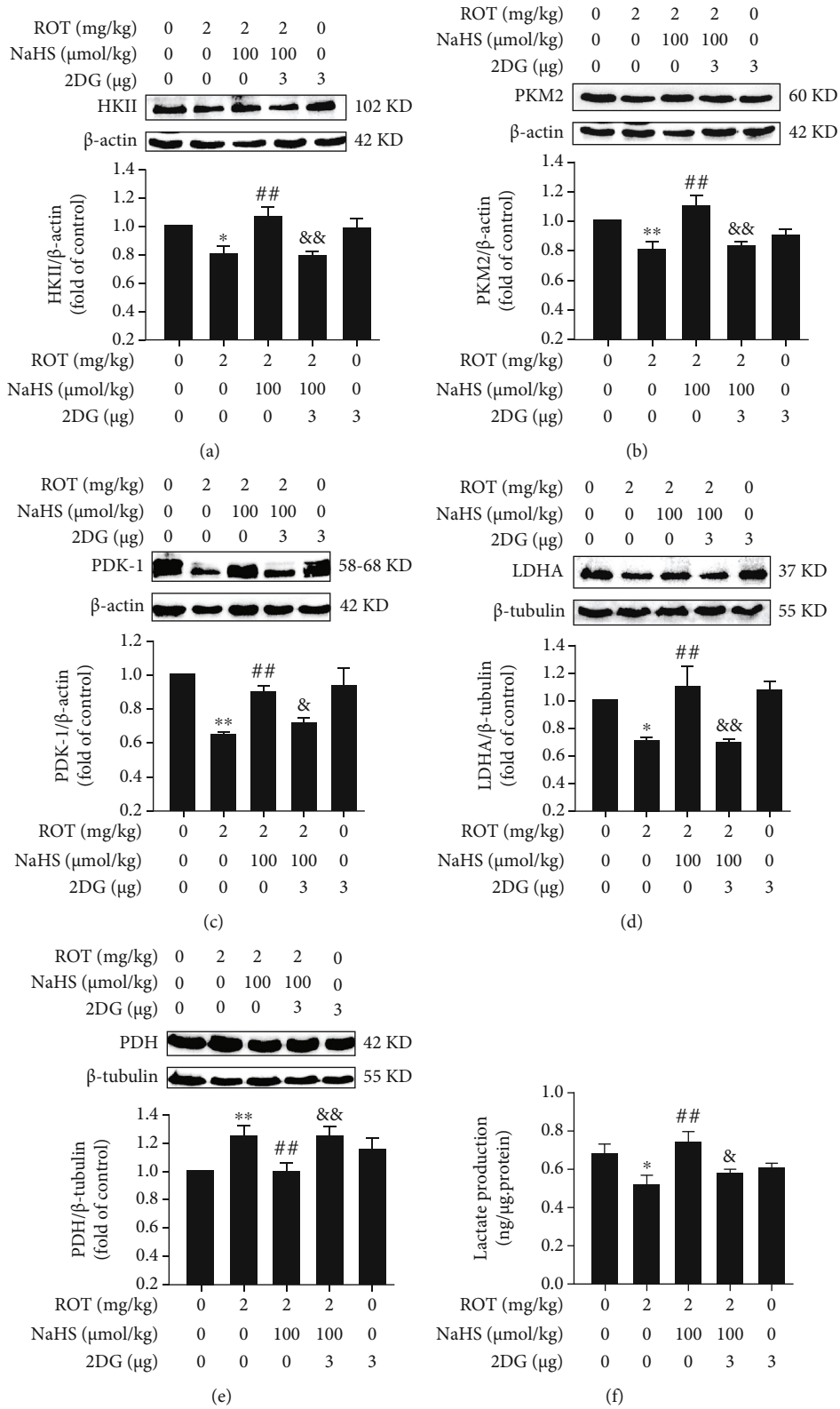

Figure 7: Effect of 2-DG on H_2S-enhanced hippocampal Warburg effect in ROT-treated rats. After pretreatment with NaHS (100 μmol/kg, i.p.) for 1 w, SD rats were injected with ROT (2 mg/kg, s.c.) for 5 w. In the 3rd week of injecting ROT, rats were cotreated with NaHS (100 μmol/kg, i.p.) and 2-DG (3 μg/w, i.c.v.) for 3 w simultaneously. The expressions of HKII (a), PKM2 (b), PDK-1 (c), LDHA (d), and PDH (e) in the hippocampus were detected by western blot. The content of lactate (f) in the hippocampus was tested by a lactate assay kit. Values are presented as the mean ± S.E.M. ($n = 3$). $^{*}P < 0.05$ and $^{**}P < 0.01$ vs. control group; $^{\#\#}P < 0.01$ vs. ROT treatment alone group; $^{\&}P < 0.05$ and $^{\&\&}P < 0.01$ vs. ROT and NaHS cotreatment groups.

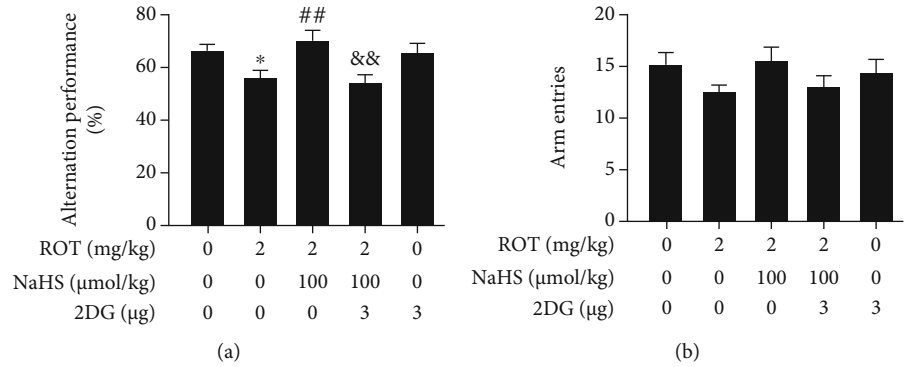

Figure 8: Effect of 2-DG on H_2S-ameliorated cognitive impairment of ROT-exposed rats in the Y-maze test. After pretreatment with NaHS (100 μmol/kg, i.p.) for 1 w, SD rats were injected with ROT (2 mg/kg, s.c.) for 5 w. In the 3rd week of ROT injection, rats were cotreated with NaHS (100 μmol/kg, i.p.) and 2-DG (3 μg/w, i.c.v.) for 3 w simultaneously. All rats were subjected to the Y-maze test. The alternation performance (a) and arm entries (b) over the course of 5 min were analyzed. Values are presented as the mean ± S.E.M. ($n = 9 – 15$). $^{*}P < 0.05$ vs. control group; $^{\#\#}P < 0.01$ vs. ROT treatment alone group; $^{\&\&}P < 0.01$ vs. ROT and NaHS cotreatment groups.

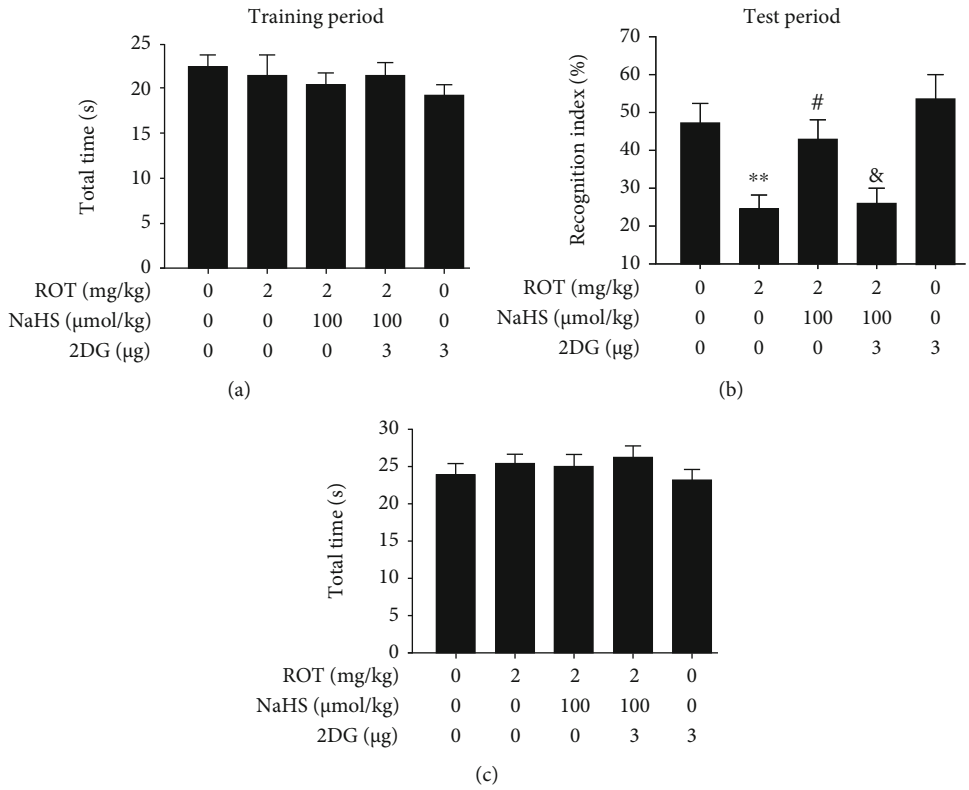

Figure 9: Effect of 2-DG on H_2S-ameliorated cognitive impairment of ROT-induced PD rats in the NOR test. After pretreatment with NaHS (100 μmol/kg, i.p.) for 1 w, SD rats were injected with ROT (2 mg/kg, s.c.) for 5 w. In the 3rd week of ROT injection, rats were cotreated with NaHS (100 μmol/kg, i.p.) and 2-DG (3 μg/w, i.c.v.) for 3 w simultaneously. All rats were subjected to the NOR test. The total time in the training period (a) and recognition index (b) as well as the total time (c) in the test period over the course of 5 min were recorded. Values are presented as the mean ± S.E.M. ($n = 9 – 15$). $^{**}P < 0.01$ vs. control group; $^{\#}P < 0.05$ vs. ROT treatment alone group; $^{\&}P < 0.05$ vs. ROT and NaHS cotreatment groups.

dramatically enhanced the learning and memory as well as the hippocampal microglia M2 polarization in the ROT-induced PD rats. H_2S also promoted the hippocampal Warburg effect in the ROT-induced PD rats. Moreover, inhibition of the Warburg effect in the hippocampus significantly reversed H_2S-promoted cognitive function and hippocampal microglia M2 polarization in the ROT-induced PD rats. Our findings identify H_2S as a potential innovative inhibitor of cognitive deficit in PD and suggest that this effect is achieved via promoting microglia M2 polarization by upregulation of Warburg effect in the hippocampus.

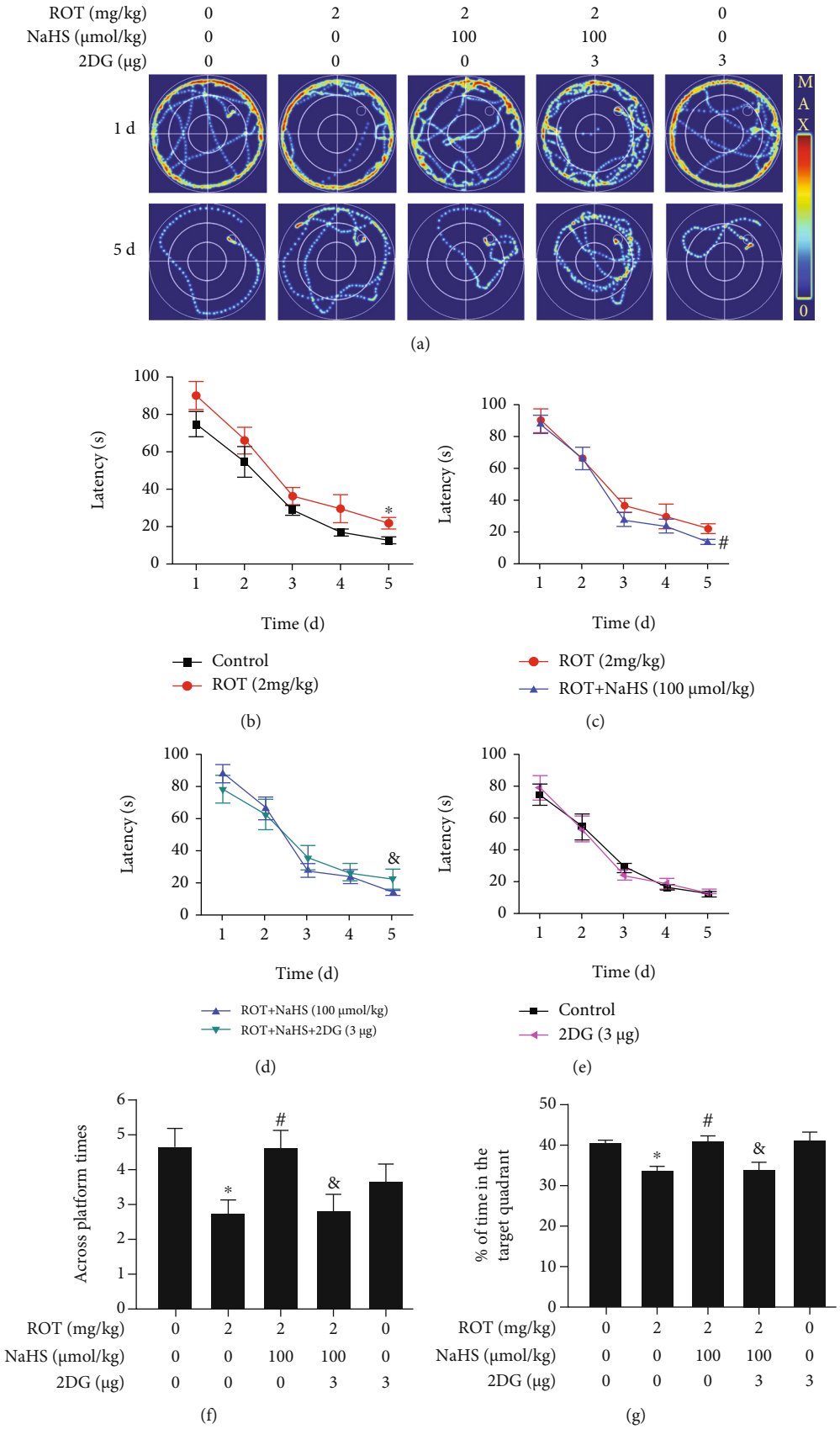

Figure 10: Continued.

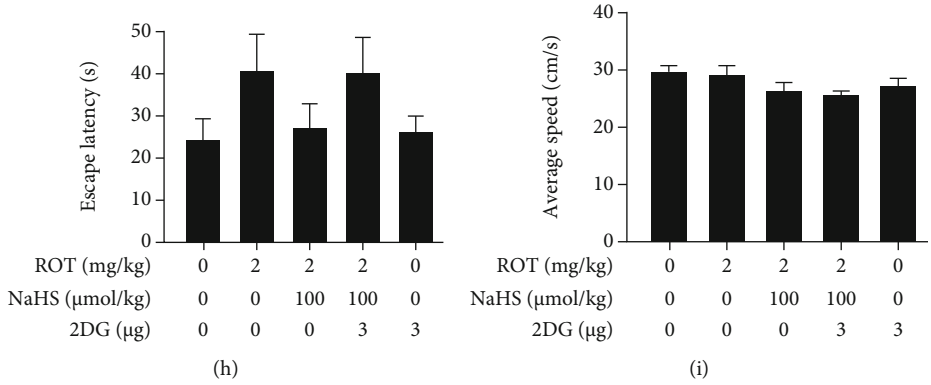

FIGURE 10: Effect of 2-DG on H_2S-ameliorated cognitive dysfunction of ROT-induced PD rats in the MWM test. After pretreatment with NaHS (100 μmol/kg, i.p.) for 1 w, SD rats were injected with ROT (2 mg/kg, s.c.) for 5 w. In the 3rd week of ROT injection, rats were cotreated with NaHS (100 μmol/kg, i.p.) and 2-DG (3 μg/w, i.c.v.) for 3 w simultaneously. The representative swimming routes of one rat for each group in searching for the platform were recorded on the 1st and 5th training days (a). The latency to find the platform in the acquisition phase was recorded (b–e). The number across platform (f) and the percentage of time spent in the target quadrant (g) in the probe trial phase were recorded. The escape latency (h) and average speed (i) of rats in the visible platform phase were recorded. Values are presented as the mean ± S.E.M. ($n = 9 - 15$). $^{*}P < 0.05$ vs. control group; $^{\#}P < 0.05$ vs. ROT treatment alone group; $^{\&}P < 0.05$ vs. ROT and NaHS cotreatment groups.

PD is one of the most familiar neurodegenerative diseases in the clinic, featuring motor and nonmotor disorders [36, 37]. Dementia, a nonmotor symptom, develops in the early stage of PD. Increasing studies using animal models have verified that H_2S recovers the number of dopaminergic neurons to normal and mitigates motor disorders [38, 39], identifying H_2S as a new hope for the treatment of PD [40]. As a novel gaseous signaling molecule, H_2S has the capacity to attenuate deficits in learning and memory induced by risk factors [16, 17, 41]. Accordingly, our study is aimed at investigating whether H_2S protects against the cognitive impairment in ROT-induced PD rats. In the Y-maze test, we found that NaHS supplementation markedly increased alternation performance in ROT-exposed rats, suggesting a benefit of H_2S to the cognitive function of ROT-exposed rats. In the NOR test, the declined recognition index in ROT-treated rats was reversed by the administration of NaHS, which indicated that H_2S ameliorates deficits in learning and memory in ROT-treated rats. In the MWM test, NaHS greatly shortened the escape latency in the acquisition phase and increased the number of crossing platform as well as the time spent in the target quadrant in the probe trial of ROT-exposed rats, which further suggested that the impairment in spatial learning and memory in ROT-treated rats is reversed by H_2S. Collectively, our data demonstrate that H_2S prevents cognitive dysfunction in ROT-induced PD rats. It has demonstrated that H_2S reduces neurodegeneration in MPP^+-, ROT-, and 6-hydroxydopamine (6-OHDA)-caused PD models [42–44]. Thus, we believe that H_2S holds promise for providing therapeutic benefits in the cognitive impairment of PD.

Microglia is the first line of defense of the central nervous system in the resting condition; microglia not only provide surveillance but also respond to danger signals [45]. Activated microglia exhibits two different statuses, M1 and M2. A previous study revealed microglia activation in the hippocampus of PD patients [46]. Furthermore, microglia play a crucial role in neuronal plasticity and neurogenesis [19, 47]. The hippocampus, one of limbic system structures, is well known in learning and memory. It also has been reported that hippocampus lesion contributes to memory dysfunction [4, 5], and reversing hippocampal volume loss improves memory function [6]. Cognitive impairment and hippocampal atrophy are hallmark features in PD patients, and hippocampal atrophy is reported to predict PD dementia [48, 49]. Microglia polarization is known to influence cognitive function and has therefore become a main player in neurodegenerative diseases leading to dementia. It has been reported that young offspring rats with cognitive impairment after maternal sleep deprivation exposure exhibit increase in microglia activation and M1 phenotype of microglia as well as a decrease in M2 phenotype of microglia [50]. Suppressing microglia M1 polarization in the hippocampus is an important mechanism in protecting against chronic unpredictable mild stress-induced cognitive disturbance [51]. Similarly, promoting microglia M2 polarization is able to ameliorate cognitive deficits in AD mice [52]. Inspiringly, inhibition of hippocampal microglial activation alleviates cognitive impairment in a PD model [53]. Therefore, the microglia polarization in the hippocampus was focused in the cognitive decline of PD. There are increased activation and M1 phenotype of microglia and decreased M2 phenotype of microglia in the hippocampus of ROT-treated rats. Therefore, we suggested that the cognitive deficit in PD model is also closely related to increased M1 polarization and reduced M2 polarization of microglia in the hippocampus. Notably, supplementation of NaHS significantly promoted hippocampal microglia M2 polarization in ROT-induced PD rats. Moreover, enhancing endogenous H_2S via overexpression of cystathionine β-synthase promotes M2 polarization in lipopolysaccharide- [54] or ROT- [26] stimulated microglia. Similarly, exogenous H_2S application with NaHS evokes the M2 polarization of ROT-exposed primary microglia [26]. Collectively, our data

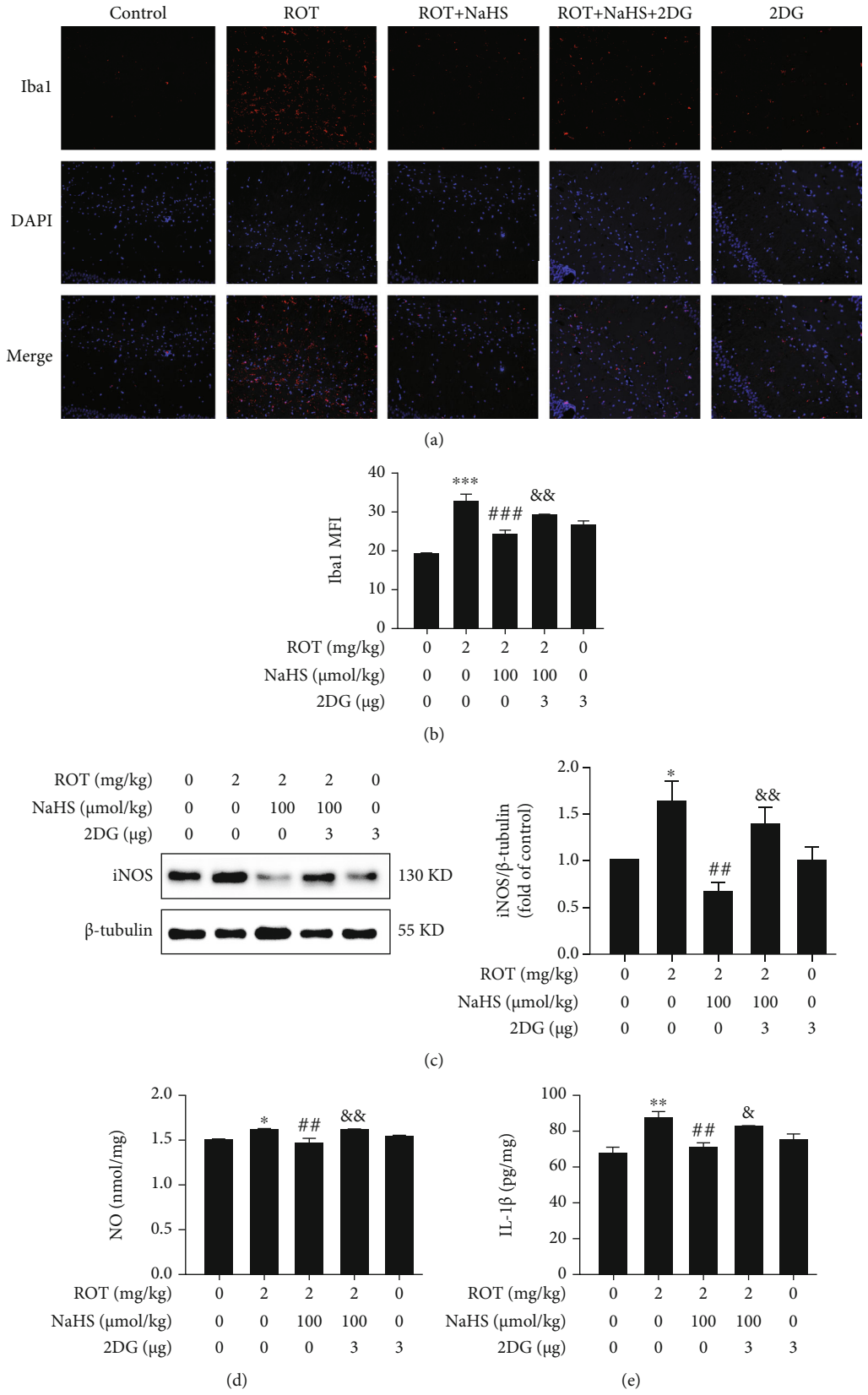

Figure 11: Continued.

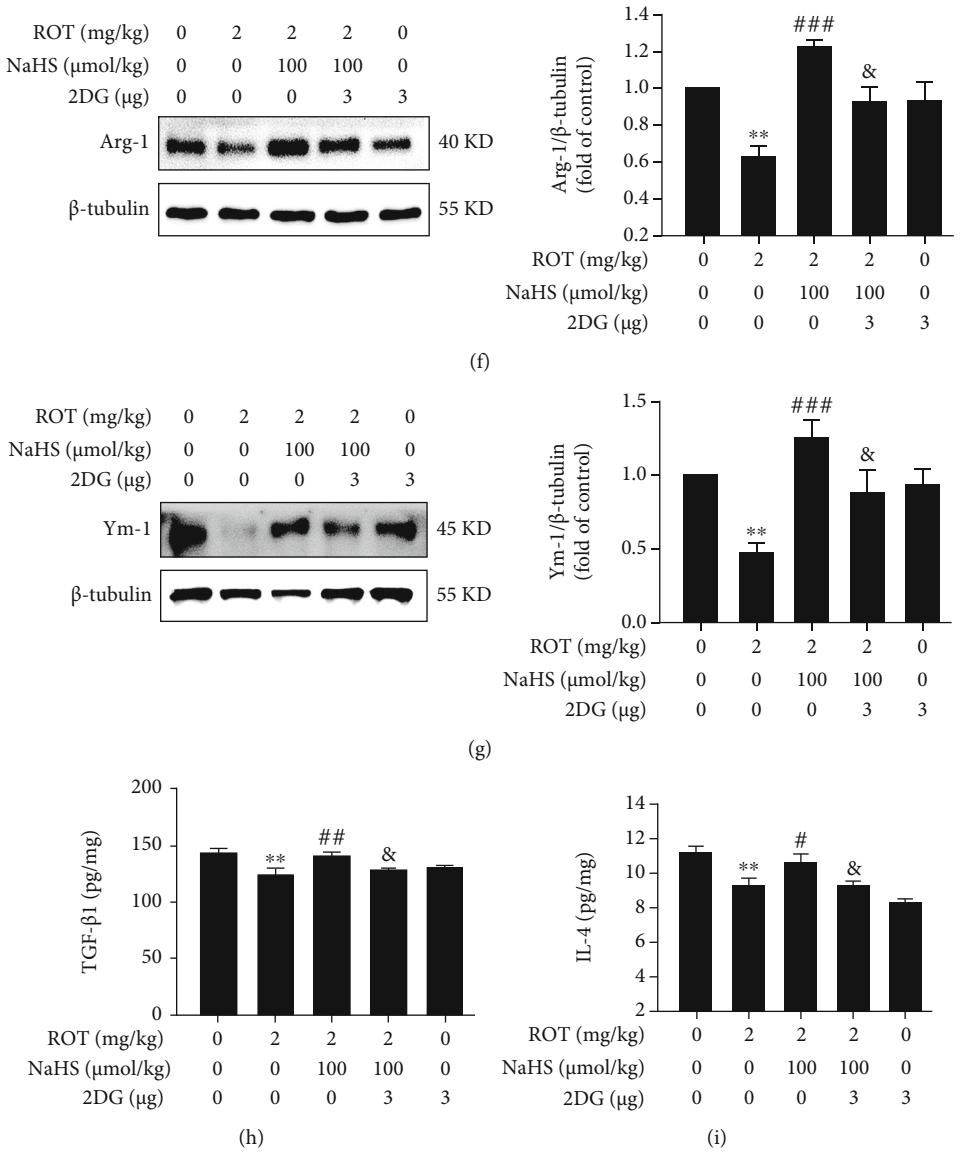

Figure 11: Effect of 2-DG on H_2S-promoted microglia M2 polarization in ROT-exerted PD rats. After pretreatment with NaHS (100 μmol/kg, i.p.) for 1 w, SD rats were injected with ROT (2 mg/kg, s.c.) for 5 w. On the 3rd w of injecting ROT, rats were cotreated with NaHS (100 μmol/kg, i.p.) and 2-DG (3 μg/w, i.c.v.) for 3 w simultaneously. Representative images of activated microglia (a). Quantitation of mean fluorescence intensity (MFI) of Iba1 (b). The nuclei were stained by DAPI (blue), and the activated microglia was stained by Iba1 (red). Magnification, 20x. The expressions of iNOS (c), Arg-1 (f), and Ym-1 (g) were measured by western blot. The level of NO (d) was measured by the Griess assay kit. The contents of IL-1β (e), TGF-β1 (h), and IL-4 (i) were detected by ELISA. Values are presented as the mean ± S.E.M. ($n = 3$). $^{*}P < 0.05$, $^{**}P < 0.01$, and $^{***}P < 0.001$ vs. control group; $^{\#}P < 0.05$, $^{\#\#}P < 0.01$, and $^{\#\#\#}P < 0.001$ vs. ROT treatment alone group; $^{\&}P < 0.05$ and $^{\&\&}P < 0.01$ vs. the ROT and NaHS cotreatment groups.

suggest the critical role of promoting hippocampal microglia M2 polarization in H_2S-exerted protection against the cognitive dysfunction in PD. Microglia polarization occupies an important role in cognitive function and it is worth exploring deeply. Our future studies in this exciting and growing field will continue to reveal the effects of microglia in other brain regions on the cognitive impairment in PD.

The Warburg effect, or aerobic glycolysis, is an energy metabolism shift to glycolysis under aerobic conditions. This phenomenon was first discovered in cancer by Otto Warburg [55]. Besides supplying energy quickly, the Warburg effect serves as a vital characteristic of nontumor disease, especially in neurodegenerative disease [56, 57]. Increasing the expression of HKII attenuates ROT-induced cell death [58]. Corona et al. confirmed that an elevated Warburg effect in the brain reduces the amount of dopaminergic neuron death and improves PD symptoms [59]. More importantly, the Warburg effect maintains LTP and regulates synaptic reconstruction, resulting in an enhancement in learning and memory [30, 32]. Thus, there is a scientific research value to elucidate the mechanism underlying H_2S-attenuated cognitive impairment in the ROT-exposed rats

from the new perspective of the hippocampal Warburg effect. We found that the expressions of HKII, PKM2, PDK-1, and LDHA and the content of lactate in the hippocampus of ROT-treated rats were decreased, while the expression of PDH was increased. All these data indicated the downregulation of the hippocampal Warburg effect in ROT-exposed rats. Recent evidence confirmed that downregulation of Warburg effect via dichloroacetate impairs the learning and memory in mice [60], suggesting a requirement of Warburg effect for spatial memory acquisition. Furthermore, Shannon et al. also support the contribution of brain Warburg effect to learning [61]. In the present work, we demonstrated that H_2S increased the hippocampal Warburg effect in ROT-exposed rats and that inhibited Warburg effect reversed the protection of H_2S against cognitive dysfunction in ROT-exposed rats. Collectively, enhancing hippocampal Warburg effect plays a crucial role in H_2S-provided therapeutic benefits in the cognitive impairment of PD.

Immune cells need different amounts of energy to exert various functions, and the metabolic pathways responsible for energy generation are determined by cellular phenotypes [62]. Under the classical inflammatory activation process (M1), microglia often undergo metabolic reprogramming toward aerobic glycolysis. In comparison, microglia with M2 status induced by IL-4 stimulation exhibit decreased lactate release and glucose consumption, suggesting reduced aerobic glycolysis [63, 64]. 2-DG, an inhibitor of HKII, is widely used to downregulate the Warburg effect [65], which was also confirmed in our study. More interestingly, 2-DG blunts the release of M1 polarization-associated markers TNF-α and IL-6 in primary microglia [66]. Given the link between microglia polarization and energy metabolism, whether the Warburg effect-mediated M2 microglia polarization contributes to H_2S-produced neuroprotection in cognitive disorder is worth to research. From our data, 2-DG reversed the reduced M1 markers and the increased M2 markers in the hippocampal microglia by NaHS in ROT-induced PD rats, representing a microglia transition from M2 to M1. Additionally, 2-DG dramatically reversed H_2S the attenuated cognitive deficits in the ROT-induced PD rats. In summary, our findings verified that H_2S enhances the hippocampal Warburg effect to accelerate microglia polarization toward M2, which consequently ameliorates cognitive impairment.

Taken together, our findings demonstrated that H_2S produces a protective response to the cognitive dysfunction of PD as a result of elevated microglia M2 polarization via enhancing the hippocampal Warburg effect. This study elucidates a previously unrecognized mechanism in the antagonistic effect of H_2S on cognitive deficits and thereby provides a strong basis for the development of therapeutics targeting H_2S bioavailability or the Warburg effect in the treatment of comorbid cognitive disorder and PD that is refractory to current drugs. Additionally, it is necessary to make effort to clarity the pathologic alteration in Parkinson's cognitive dysfunction. We will pay more attention to the relationship between pathologic alteration and microglia activation in our next step.

Data Availability

The datasets analyzed during the current study are available from the corresponding authors upon reasonable request.

Ethical Approval

All experiments strictly complied with the *Guide for the Care and Use of Laboratory Animals* of the National Institutes of Health and were approved by the Animal Use and Protection Committee of the University of South China.

Conflicts of Interest

The authors declare that they have no competing interests.

Authors' Contributions

XQT and PZ were responsible for research design. QT, HLT, and YYT performed the experiments. PZ, XK, and WZ collected and analyzed the data. QT, YYT, and HLT wrote or contributed to the writing of the manuscript. XQT reviewed the data and modified the manuscript. The authors read and approved the final manuscript. Qing Tian, Hui-Ling Tang, and Yi-Yun Tang contributed equally to this work.

Acknowledgments

This work was supported by the National Natural Science Foundation of China (81771178), the Natural Science Foundation of Hunan Province (2020JJ4553), and the Clinical Medical Technology Innovation Guidance Project of Hunan Province (2020SK51908).

References

[1] D. J. Moore, A. B. West, V. L. Dawson, and T. M. Dawson, "Molecular pathophysiology of Parkinson's disease," *Annual Review of Neuroscience*, vol. 28, no. 1, pp. 57–87, 2005.

[2] T. Li and W. Le, "Biomarkers for Parkinson's disease: how good are they?," *Neuroscience Bulletin*, vol. 36, no. 2, pp. 183–194, 2020.

[3] A. H. V. Schapira, K. R. Chaudhuri, and P. Jenner, "Non-motor features of Parkinson disease," *Nature Reviews. Neuroscience*, vol. 18, no. 7, pp. 435–450, 2017.

[4] T. D. Miller, T. T.-J. Chong, A. M. Aimola Davies et al., "Human hippocampal CA3 damage disrupts both recent and remote episodic memories," *Elife*, vol. 9, 2020.

[5] M. M. Albasser, E. Amin, T. C. Lin, M. D. Iordanova, and J. P. Aggleton, "Evidence that the rat hippocampus has contrasting roles in object recognition memory and object recency memory," *Behavioral Neuroscience*, vol. 126, no. 5, pp. 659–669, 2012.

[6] K. I. Erickson, M. W. Voss, R. S. Prakash et al., "Exercise training increases size of hippocampus and improves memory," *Proceedings of the National Academy of Sciences of the United States of America*, vol. 108, pp. 3017–3022, 2011.

[7] M. K. Beyer, K. S. Bronnick, K. S. Hwang et al., "Verbal memory is associated with structural hippocampal changes in newly diagnosed Parkinson's disease," *Journal of Neurology, Neurosurgery, and Psychiatry*, vol. 84, no. 1, pp. 23–28, 2013.

[8] A. Low, H. Foo, T. T. Yong, L. C. S. Tan, and N. Kandiah, "Hippocampal subfield atrophy of CA1 and subicular structures predict progression to dementia in idiopathic Parkinson's disease," *Journal of Neurology, Neurosurgery, and Psychiatry*, vol. 90, no. 6, pp. 681–687, 2019.

[9] K. Abe and H. Kimura, "The possible role of hydrogen sulfide as an endogenous neuromodulator," *The Journal of Neuroscience*, vol. 16, no. 3, pp. 1066–1071, 1996.

[10] H. J. Huang, S. L. Chen, and H. M. Hsieh-Li, "Administration of NaHS attenuates footshock-induced pathologies and emotional and cognitive dysfunction in triple transgenic Alzheimer's mice," *Frontiers in Behavioral Neuroscience*, vol. 9, 2015.

[11] S. A. Karimi, N. Hosseinmardi, M. Janahmadi, M. Sayyah, and R. Hajisoltani, "The protective effect of hydrogen sulfide (H_2S) on traumatic brain injury (TBI) induced memory deficits in rats," *Brain Research Bulletin*, vol. 134, pp. 177–182, 2017.

[12] X. Hu, L. Luan, W. Guan et al., "Hydrogen sulfide attenuates isoflurane-induced neuroapoptosis and cognitive impairment in the developing rat brain," *BMC Anesthesiology*, vol. 17, p. 123, 2017.

[13] X.-Q. Tang, Y.-Y. Zhuang, P. Zhang et al., "Formaldehyde impairs learning and memory involving the disturbance of hydrogen sulfide generation in the hippocampus of rats," *Journal of Molecular Neuroscience*, vol. 49, pp. 140–149, 2013.

[14] M.-H. Li, J.-P. Tang, P. Zhang et al., "Disturbance of endogenous hydrogen sulfide generation and endoplasmic reticulum stress in hippocampus are involved in homocysteine-induced defect in learning and memory of rats," *Behavioural Brain Research*, vol. 262, pp. 35–41, 2014.

[15] M. Li, P. Zhang, H.-j. Wei et al., "Hydrogen sulfide ameliorates homocysteine-induced cognitive dysfunction by inhibition of reactive aldehydes involving upregulation of ALDH2," *The International Journal of Neuropsychopharmacology*, vol. 20, pp. 305–315, 2017.

[16] Y.-Y. Tang, A.-P. Wang, H.-J. Wei et al., "Role of silent information regulator 1 in the protective effect of hydrogen sulfide on homocysteine-induced cognitive dysfunction: involving reduction of hippocampal ER stress," *Behavioural Brain Research*, vol. 342, pp. 35–42, 2018.

[17] X.-N. Li, L. Chen, B. Luo et al., "Hydrogen sulfide attenuates chronic restrain stress-induced cognitive impairment by upreglulation of Sirt1 in hippocampus," *Oncotarget*, vol. 8, pp. 100396–100410, 2017.

[18] W. Zou, J. Yuan, Z.-J. Tang et al., "Hydrogen sulfide ameliorates cognitive dysfunction in streptozotocin-induced diabetic rats: involving suppression in hippocampal endoplasmic reticulum stress," *Oncotarget*, vol. 8, pp. 64203–64216, 2017.

[19] L. Sominsky, S. De Luca, and S. J. Spencer, "Microglia: key players in neurodevelopment and neuronal plasticity," *The International Journal of Biochemistry & Cell Biology*, vol. 94, pp. 56–60, 2018.

[20] M. Cowan and W. A. Petri Jr., "Microglia: immune regulators of neurodevelopment," *Frontiers in Immunology*, vol. 9, p. 2576, 2018.

[21] L. Cao and C. He, "Polarization of macrophages and microglia in inflammatory demyelination," *Neuroscience Bulletin*, vol. 29, no. 2, pp. 189–198, 2013.

[22] H. J. Park, S. H. Oh, H. N. Kim, Y. J. Jung, and P. H. Lee, "Mesenchymal stem cells enhance α-synuclein clearance via M2 microglia polarization in experimental and human parkinsonian disorder," *Acta Neuropathologica*, vol. 132, no. 5, pp. 685–701, 2016.

[23] K. S. MacDowell, E. Munarriz-Cuezva, J. R. Caso et al., "Paliperidone reverts Toll-like receptor 3 signaling pathway activation and cognitive deficits in a maternal immune activation mouse model of schizophrenia," *Neuropharmacology*, vol. 116, pp. 196–207, 2017.

[24] D. Zhu, N. Yang, Y. Y. Liu, J. Zheng, C. Ji, and P. P. Zuo, "M2 macrophage transplantation ameliorates cognitive dysfunction in Amyloid-β-Treated rats through regulation of microglial polarization," *Journal of Alzheimer's Disease*, vol. 52, no. 2, pp. 483–495, 2016.

[25] X. Zhou, X. Chu, D. Xin et al., "L-cysteine-derived H2S promotes microglia M2 polarization via activation of the AMPK pathway in hypoxia-ischemic neonatal mice," *Frontiers in Molecular Neuroscience*, vol. 12, 2019.

[26] C. Du, M. Jin, Y. Hong et al., "Downregulation of cystathionine β-synthase/hydrogen sulfide contributes to rotenone-induced microglia polarization toward M1 type," *Biochemical and Biophysical Research Communications*, vol. 451, pp. 239–245, 2014.

[27] O. Warburg, "On the origin of cancer cells," *Science*, vol. 123, no. 3191, pp. 309–314, 1956.

[28] M. S. Goyal, M. Hawrylycz, J. A. Miller, A. Z. Snyder, and M. E. Raichle, "Aerobic glycolysis in the human brain is associated with development and neotenous gene expression," *Cell Metabolism*, vol. 19, no. 1, pp. 49–57, 2014.

[29] A. L. Bauernfeind, S. K. Barks, T. Duka, L. I. Grossman, P. R. Hof, and C. C. Sherwood, "Aerobic glycolysis in the primate brain: reconsidering the implications for growth and maintenance," *Brain Structure & Function*, vol. 219, no. 4, pp. 1149–1167, 2014.

[30] J. Yang, E. Ruchti, J.-M. Petit et al., "Lactate promotes plasticity gene expression by potentiating NMDA signaling in neurons," *Proceedings of the National Academy of Sciences of the United States of America*, vol. 111, pp. 12228–12233, 2014.

[31] C. M. Alberini, E. Cruz, G. Descalzi, B. Bessieres, and V. Gao, "Astrocyte glycogen and lactate: new insights into learning and memory mechanisms," *Glia*, vol. 66, no. 6, pp. 1244–1262, 2018.

[32] A. Suzuki, S. A. Stern, O. Bozdagi et al., "Astrocyte-neuron lactate transport is required for long-term memory formation," *Cell*, vol. 144, pp. 810–823, 2011.

[33] R. Verma and B. Nehru, "Effect of centrophenoxine against rotenone-induced oxidative stress in an animal model of Parkinson's disease," *Neurochemistry International*, vol. 55, no. 6, pp. 369–375, 2009.

[34] N. Tanimine, S. K. Germana, M. Fan et al., "Differential effects of 2-deoxy-D-glucose on in vitro expanded human regulatory T cell subsets," *PLoS One*, vol. 14, article e0217761, 2019.

[35] J. M. Rho, L.-R. Shao, and C. E. Stafstrom, "2-Deoxyglucose and beta-hydroxybutyrate: metabolic agents for seizure control," *Frontiers in Cellular Neuroscience.*, vol. 13, 2019.

[36] A. Hanganu, C. Bedetti, C. Degroot et al., "Mild cognitive impairment is linked with faster rate of cortical thinning in patients with Parkinson's disease longitudinally," *Brain*, vol. 137, pp. 1120–1129, 2014.

[37] J. B. Pereira, C. Junque, D. Bartres-Faz, B. Ramirez-Ruiz, M. J. Marti, and E. Tolosa, "Regional vulnerability of hippocampal subfields and memory deficits in Parkinson's disease," *Hippocampus*, vol. 23, no. 8, pp. 720–728, 2013.

[38] M. Lu, F.-F. Zhao, J.-J. Tang et al., "The neuroprotection of hydrogen sulfide against MPTP-induced dopaminergic neuron degeneration involves uncoupling protein 2 rather than ATP-sensitive potassium channels," *Antioxidants & Redox Signaling*, vol. 17, pp. 849–859, 2012.

[39] L. Xie, L.-F. Hu, X. Q. Teo et al., "Therapeutic effect of hydrogen sulfide-releasing L-dopa derivative ACS84 on 6-OHDA-induced Parkinson's disease rat model," *PLoS One*, vol. 8, article e60200, 2013.

[40] Y. O. Cakmak, "Rotorua, hydrogen sulphide and Parkinson's disease-a possible beneficial link?," *The New Zealand Medical Journal*, vol. 130, no. 1455, pp. 123–125, 2017.

[41] S. Ma, P. M. Di Zhong, G. Li et al., "Exogenous hydrogen sulfide ameliorates diabetes-associated cognitive decline by regulating the mitochondria-mediated apoptotic pathway and IL-23/IL-17 expression in db/db mice," *Cellular Physiology and Biochemistry*, vol. 41, pp. 1838–1850, 2017.

[42] L. F. Hu, M. Lu, Z. Y. Wu, P. T. Wong, and J. S. Bian, "Hydrogen sulfide inhibits rotenone-induced apoptosis via preservation of mitochondrial function," *Molecular Pharmacology*, vol. 75, no. 1, pp. 27–34, 2009.

[43] C. X. Tiong, M. Lu, and J. S. Bian, "Protective effect of hydrogen sulphide against 6-OHDA-induced cell injury in SH-SY5Y cells involves PKC/PI3K/Akt pathway," *British Journal of Pharmacology*, vol. 161, no. 2, pp. 467–480, 2010.

[44] X.-Q. Tang, Y.-Y. Zhuang, L.-L. Fan et al., "Involvement of K(ATP)/PI (3)K/AKT/Bcl-2 pathway in hydrogen sulfide-induced neuroprotection against the toxicity of 1-methy-4-phenylpyridinium ion," *Journal of Molecular Neuroscience*, vol. 46, no. 2, pp. 442–449, 2012.

[45] M. W. Salter and S. Beggs, "Sublime microglia: expanding roles for the guardians of the CNS," *Cell*, vol. 158, no. 1, pp. 15–24, 2014.

[46] A. Gerhard, N. Pavese, G. Hotton et al., "In vivo imaging of microglial activation with [11C](R)-PK11195 PET in idiopathic Parkinson's disease," *Neurobiology of Disease*, vol. 21, pp. 404–412, 2006.

[47] J. Zhang, X. Xie, M. Tang et al., "Salvianolic acid B promotes microglial M2-polarization and rescues neurogenesis in stress-exposed mice," *Brain, Behavior, and Immunity*, vol. 66, pp. 111–124, 2017.

[48] A. Brück, T. Kurki, V. Kaasinen, T. Vahlberg, and J. O. Rinne, "Hippocampal and prefrontal atrophy in patients with early non-demented Parkinson's disease is related to cognitive impairment," *Journal of Neurology, Neurosurgery, and Psychiatry*, vol. 75, no. 10, pp. 1467–1469, 2004.

[49] D. YILDIZ, S. ERER, M. ZARİFOĞLU et al., "Impaired cognitive performance and hippocampal atrophy in Parkinson disease," *TURKISH JOURNAL OF MEDICAL SCIENCES*, vol. 45, pp. 1173–1177, 2015.

[50] Q. Zhao, X. Xie, Y. Fan et al., "Phenotypic dysregulation of microglial activation in young offspring rats with maternal sleep deprivation-induced cognitive impairment," *Scientific Reports*, vol. 5, no. 1, 2015.

[51] X. Xu, X. Xiao, Y. Yan, and T. Zhang, "Activation of liver X receptors prevents emotional and cognitive dysfunction by suppressing microglial M1-polarization and restoring synaptic plasticity in the hippocampus of mice," *Brain, Behavior, and Immunity*, vol. 94, pp. 111–124, 2021.

[52] H. Wang, G. Peng, B. Wang et al., "IL-1R$^{-/-}$ alleviates cognitive deficits through microglial M2 polarization in AD mice," *Brain Research Bulletin*, vol. 157, pp. 10–17, 2020.

[53] K. Wang, Y. Shi, W. Liu, S. Liu, and M. Z. Sun, "Taurine improves neuron injuries and cognitive impairment in a mouse Parkinson's disease model through inhibition of microglial activation," *Neurotoxicology*, vol. 83, pp. 129–136, 2021.

[54] X. Zhou, Y. Cao, G. Ao et al., "CaMKKβ-dependent activation of AMP-activated protein kinase is critical to suppressive effects of hydrogen sulfide on neuroinflammation," *Antioxidants & Redox Signaling*, vol. 21, no. 12, pp. 1741–1758, 2014.

[55] S. J. Bensinger and H. R. Christofk, "New aspects of the Warburg effect in cancer cell biology," *Seminars in Cell & Developmental Biology*, vol. 23, no. 4, pp. 352–361, 2012.

[56] A. Vallee, Y. Lecarpentier, R. Guillevin, and J. N. Vallee, "Thermodynamics in neurodegenerative diseases: interplay between canonical WNT/beta-catenin pathway-PPAR gamma, energy metabolism and circadian rhythms," *Neuromolecular Medicine*, vol. 20, no. 2, pp. 174–204, 2018.

[57] Z. Chen, M. Liu, L. Li, and L. Chen, "Involvement of the Warburg effect in non-tumor diseases processes," *Journal of Cellular Physiology*, vol. 233, no. 4, pp. 2839–2849, 2018.

[58] A. Gimenez-Cassina, F. Lim, T. Cerrato, G. M. Palomo, and J. Diaz-Nido, "Mitochondrial Hexokinase II Promotes Neuronal Survival and Acts Downstream of Glycogen Synthase Kinase-3," *The Journal of Biological Chemistry*, vol. 284, no. 5, pp. 3001–3011, 2009.

[59] J. C. Corona, A. Gimenez-Cassina, F. Lim, and J. Diaz-Nido, "Hexokinase II gene transfer protects against neurodegeneration in the rotenone and MPTP mouse models of Parkinson's disease," *Journal of Neuroscience Research*, vol. 88, pp. NA–1950, 2010.

[60] R. A. Harris, A. Lone, H. Lim et al., "Aerobic glycolysis is required for spatial memory acquisition but not memory retrieval in mice," *eNeuro*, vol. 6, 2019.

[61] B. J. Shannon, S. N. Vaishnavi, A. G. Vlassenko, J. S. Shimony, J. Rutlin, and M. E. Raichle, "Brain aerobic glycolysis and motor adaptation learning," *Proceedings of the National Academy of Sciences of the United States of America*, vol. 113, no. 26, pp. E3782–E3791, 2016.

[62] L. A. O'Neill, R. J. Kishton, and J. Rathmell, "A guide to immunometabolism for immunologists," *Nature Reviews. Immunology*, vol. 16, no. 9, pp. 553–565, 2016.

[63] R. Orihuela, C. A. McPherson, and G. J. Harry, "Microglial M1/M2 polarization and metabolic states," *British Journal of Pharmacology*, vol. 173, no. 4, pp. 649–665, 2016.

[64] J. Gimeno-Bayon, A. Lopez-Lopez, M. J. Rodriguez, and N. Mahy, "Glucose pathways adaptation supports acquisition of activated microglia phenotype," *Journal of Neuroscience Research*, vol. 92, no. 6, pp. 723–731, 2014.

[65] J. Brown, "Effects of 2-deoxyglucose on carbohydrate metablism: review of the literature and studies in the rat," *Metabolism*, vol. 11, pp. 1098–1112, 1962.

[66] Q. Wang, Y. Zhao, M. Sun et al., "2-Deoxy-d-glucose attenuates sevoflurane-induced neuroinflammation through nuclear factor-kappa B pathway in vitro," *Toxicology In Vitro*, vol. 28, no. 7, pp. 1183–1189, 2014.